Geological Survey of Japan Cruise Report No. 22, p. 233-252, 1992

XII. MINERALOGY, CHEMISTRY, AND INTERNAL STRUCTURE OF MANGANESE NODULES IN THE SOUTHERN PART OF THE CENTRAL PACIFIC BASIN (GH82-4 AREA)

Akira Usui and Naoki Mita

Introduction

Earlier numerous chemical and mineralogical analyses have revealed significant compositional variations of manganese nodule facies in the eastern and central Pacific on regional, small scales, and microscopical scales (Andrews and Friedrich, 1979; Halbach and Özkara, 1979; Mizuno *et al.*, 1980; Usui *et al.*, 1987). However, a few studies have been made in the west and south Pacific, although several cruises have been carried out (Glasby *et al.*, 1980; Exon, 1983; Usui, 1983; Cronan, 1986). The GH82-4 area was selected after the results of Wake-Tahiti Transect survey by GSJ in 1980 (Mizuno and Nakao, 1982; Usui, 1983). The area includes a small model site (70 × 70 km), where the five-mile grid reconnaissance survey plus followed small-scale sampling were conducted to characterize regional and local variation patterns of nodule chemistry, mineralogy, and their relationships to sedimentary history.

As previously reported, chemical compositional variability is generally determined by the mode of development of the two ferromanganese minerals; buserite of early diagenetic origin and vernadite of hydrogenetic origin (Halbach *et al.*, 1975; Halbach and Özkara, 1979; Usui *et al.*, 1978; Usui, 1979a). The variation of relative content of the two ferromanganese minerals causes a strong inter-elemental correlations and close relationships between nodule chemistry and surface feature. In this aspect, mineralogical description is most important in characterizing deep-sea manganese nodules and in considering nodule growth history.

Samples and methods

One hundred and nineteen nodule samples were selected from 112 stations of nodule occurrence in this area. Each sample from one station includes a half to several entire nodules so that they may represent approximate mean bulk characteristics. Described nodules were split and polished for ore microscopy, one half was ground into powder and divided into three parts for X-ray powder diffraction analysis (XRD), chemical analysis, and water content determination. Nine elements, Mn, Fe, Cu, Ni, Co, Pb, Zn, Si, and Al, were determined by atomic absorption spectroscopy (AA) according to analytical guideline of GSJ (Terashima, 1978; Mochizuki and Terashima, 1983). Water contents were determined as H_2O+ by Penfield Method and H_2O- by

Keywords: mineralogy, chemistry, internal structure, microscopy, X-ray diffraction, buserite, vernadite, Central Pacific Basin, Hakurei-Maru, Nova-Canton Trough

drying in oven.

Mineral composition was determined by XRD and/or microscopy. XRD was accomplished in a constant measuring condition by using a diffractometer Type RAD-rA (Rigaku Denki Co. Ltd.) Peak heights were measured at 10 and 2.4 Å d-spacings for quantitative estimation of mineral components; 10 and 5 Å d-spacings are diagnostic of buserite, but 2.4 Å and 1.4 Å reflections are responsible both to buserite and vernadite (δ-MnO_2). Accessory silicate minerals, phosphates, carbonates etc. were examined and estimated in comparison with ASTM and JCPDS data files.

Microscopic identification was also available in identifying ferromanganese minerals and for description of internal microstructure. The criteria for mineral identification follows after Usui (1979a).

Mineral composition

Because of low crystallinity, fine particle size, and hydrous nature, mineralogy of marine ferromanganese minerals is still controversial. Terminology is even complicated; for instance, nodule 10 Å mineral (diagnostic of 10 Å d-spacing on XRD) may be named *10 Å manganite, 10 Å manganate, buserite, todorokite* (Burns and Burns, 1977; Giovanoli, 1980; Burns *et al.*, 1983; Ostwald, 1984). In this article, nodule 10 Å manganese mineral is called as *buserite*, and the other low-crystalline ferromanganese mineral is called *vernadite*. Typical X-ray diffraction patterns of the two minerals are shown in Figure XII-1. The relative mineral contents are listed in Table XII-1, together with chemical composition and nodule morphological type. Semi-quantitative XRD analysis shows that only buserite and vernadite are principal ferromanganese minerals of GH82-4 nodules. The 7 Å mineral (so-called *birnessite*) was not detected from any nodules from this area. The occurrence of minerals are similar to those of our previous studies in the northern Central Pacific Basin nodules and the earlier works on the northeastern equatorial Pacific nodules (Cronan, 1980; Piper *et al.*, 1977).

As mentioned in chapter X (Usui, this volume), morphology of nodules of this area is variable on a scale of kilometers within the detailed survey area. Surface morphology (rough or smooth structures) is again closely related with mineralogy as revealed in earlier works (Usui, 1979a, 1979b; Usui, 1983; Usui *et al.*, 1987); that is, rough structure consists of buserite while smooth structure of vernadite. However, bulk chemical and mineral composition is not necessarily closely related with surface feature, because of variable mineral composition inside the nodules in some cases.

Manganese-free accessory minerals in the nodules are quartz, plagioclase, phillipsite, and smectite. These silicate minerals may have been incorporated into nodules, as settling particles, as nuclei, or as inclusion of surface sediment. Quartz is most common and shows two- to three-fold variation in contents, although its contents does not vary concordantly with nodule morphological type. Phillipsite seems to be associated with s-type nodules as brownish claystone in nuclei or inclusion. Smectite is also associated with the claystones.

Bulk chemical characteristics

Concentrations of major and minor metal elements of manganese nodules of this

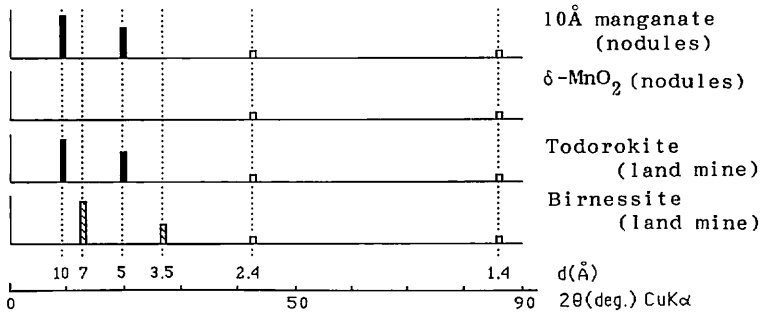

Fig. XII-1 Schematic X-ray diffraction patterns of manganese nodule minerals, land todorokite, and birnessite. Black bars denote the peaks responsible for buserite, the hatched for 7 Å manganate, and the blank for vernadite and above two minerals.

area are within the range of typical Pacific deep-sea nodules (Hein, 1977; Frazer and Fisk, 1981; Sorem *et al.*, 1979; Mckelvy, 1986). The average of nickel plus copper grade is around 2.0 wt.%, which is comparable to that of high-grade nodules from the Northeastern Equatorial Manganese Nodule Belt. When converted to oxides (as MnO_2, Fe_2O_3, CuO, NiO, Co_2O_3, PbO_2, ZnO, SiO_2, Al_2O_3, H_2O+), the analyses of nodules sum to between 85 to 91 wt.%. Manganese is always a major element ranging from 8 to 33 wt.%, whereas iron is much less. It is notable that minor metal elements are strongly correlated with either Mn or Fe. The elements, Cu, Ni, and Zn are positively correlated with Mn, but Co and Pb are correlated with Fe. A positive correlation within Mn-Cu-Ni-Zn is related with buserite, and a correlation within Fe-Co-Pb related with vernadite. Si and Al, mutually correlated, seem to vary independently with the two manganese minerals.

Earlier chemical and mineralogical studies (Usui *et al.*, 1978; Halbach and Özkara, 1979; Usui, 1979a, 1979b) have concluded that the principal mineral components of deep-sea manganese nodules are as follows; 1) buserite phase: iron-free and nearly stoichiometric hydrous manganate mineral, containing lattice-held Cu, Ni and Zn. The atomic ratio (Cu+Ni+Zn)/Mn falls on around 0.16 (nearly equal to 1/6) or slightly less. The phase forms rough microstructure as cusps or dendrites on the surface or within nodules. It is precipitated as manganate (Mn^{4+}) mineral after oxidation of dissolved manganese (Mn^{2+}) from interstitial water of unconsolidated surface sediments in the course of early diagenesis of the sediments. Minor essential elements (Cu, Ni, Zn) are subsequently incorporated between sheet structure after ion exchange, 2) vernadite phase: poorly-crystallized mixed-layer mineral (two X-ray reflections) composed of hydrous manganese oxide and ferric oxides, which amounts similar Mn and Fe. Minor elements, Cu, Ni and Zn are much more depleted. The mineral forms smooth surfaces as stratified layers with occasional columnar patterns. It is deposited from settling colloidal particles of oxides from overlying oxygenated sea water, 3) Mn-free silicate minerals: fine particles of clay minerals, zeolites, plagioclases, quartz, fossils, etc. in oxide layers and nuclei.

The nodule surface feature, mineralogy, and chemical composition are therefore closely related. In case microstructure and mineralogy do not vary on and within nodules, the type-r nodule is high in Mn, Cu, Ni, Zn, and Mn/Fe and low in Fe, Co, Pb., while the type-s nodules are vice versa. As shown in Table XII-2, the nodule bulk composition is markedly related to morphological type, reflecting their mineral composition. All parameters except for Mn, Si and Al increase or decrease in the order of type-r, intermediate type, and type-s.

Inter-element correlations are well explained based on mineral composition. The two major elements, Mn and Fe, are weakly negatively correlated and of scattered pattern due to variable content of non-manganese minerals (Fig. XII-2A). The plots of Cu+Ni+Zn versus 10 Å reflection intensity show a strong linear dependency to buserite abundance ($r = +0.96$), and the regression line may be extrapolated to the zero point (Fig. XII-2C). However, the plots of Cu+Ni+Zn versus Mn shows a relatively linear pattern (correlation coefficient $r = +0.84$), but its extrapolation suggests some fraction of Mn is not related to Cu+Ni+Zn (Fig. XII-2B). This is also due to preferential concentration between two minerals.

The ratio Fe/Mn must be linearly dependent of relative abundance of vernadite to the both minerals ideally. Total Cu+Ni+Zn is therefore expected to vary as a hyperbolic function of its reciprocal Mn/Fe. Figure XII-2D well supports this interpretation. Co concentrated in vernadite is positively correlated with Fe (Fig. XII-2F) probably exchanging Mn^{4+} or Fe^{3+} sites of the mineral.

The cluster analysis (Fig. XII-3) based on correlation coefficient matrix (Table XII-3) demonstrates clearly classified three groups of components : 1) buserite, Mn, Cu, Ni, and Zn, 2) vernadite, Fe, Co and Pb, 3) silicate minerals and Si, Al. The three groups are again consistent with the mineralogical interpretation. In the Bonatti's ternary diagram (Bonatti *et al.*, 1972) the total Cu, Ni and Zn is again linearly dependent of Mn and Fe concentrations for nodules (Fig. XII-4A). The two intersections of an extrapolated regression line and triangle axes are regarded as the ideal compositions of the two minerals. The ratio among Cu/Ni/Zn is fairly constant and irrespective of nodule type, minerals, or locality (Fig. XII-4B). The ratio is very similar to that found in the GH81-4 (Usui and Terashima, 1986) to the north of this area.

The considerably high contents of Si and Al are attributable to silicate minerals in nodule nuclei and detrital particles which are commonly observed under microscope. The sum SiO_2 and Al_2O_3 mostly falls on the range between 18 and 25 wt.%, with occasional abundance. Plots of Si versus Al show a strong positive correlation crossing near the zero point (Fig. XII-2F). The mean atomic ratio Si/Al of these nodules is around 2.7 ranging from 2.2 to 3.2. This value covers the composition for marine phillipsite (2.4 to 2.8; Boles, 1977).

Local variation of chemistry and mineralogy

GH82-4 nodules are characteristic of great local variability in chemical composition as most distinctly represented by a ratio Mn/Fe. The ratio varies from 0.7 to 5.5. The wide range of variation of the two major elements is comparable to those observed on regional scale in the world oceans. When combined with above-mentioned mineral analyses, this variation is ascribed to contents of the two mineral components. That is,

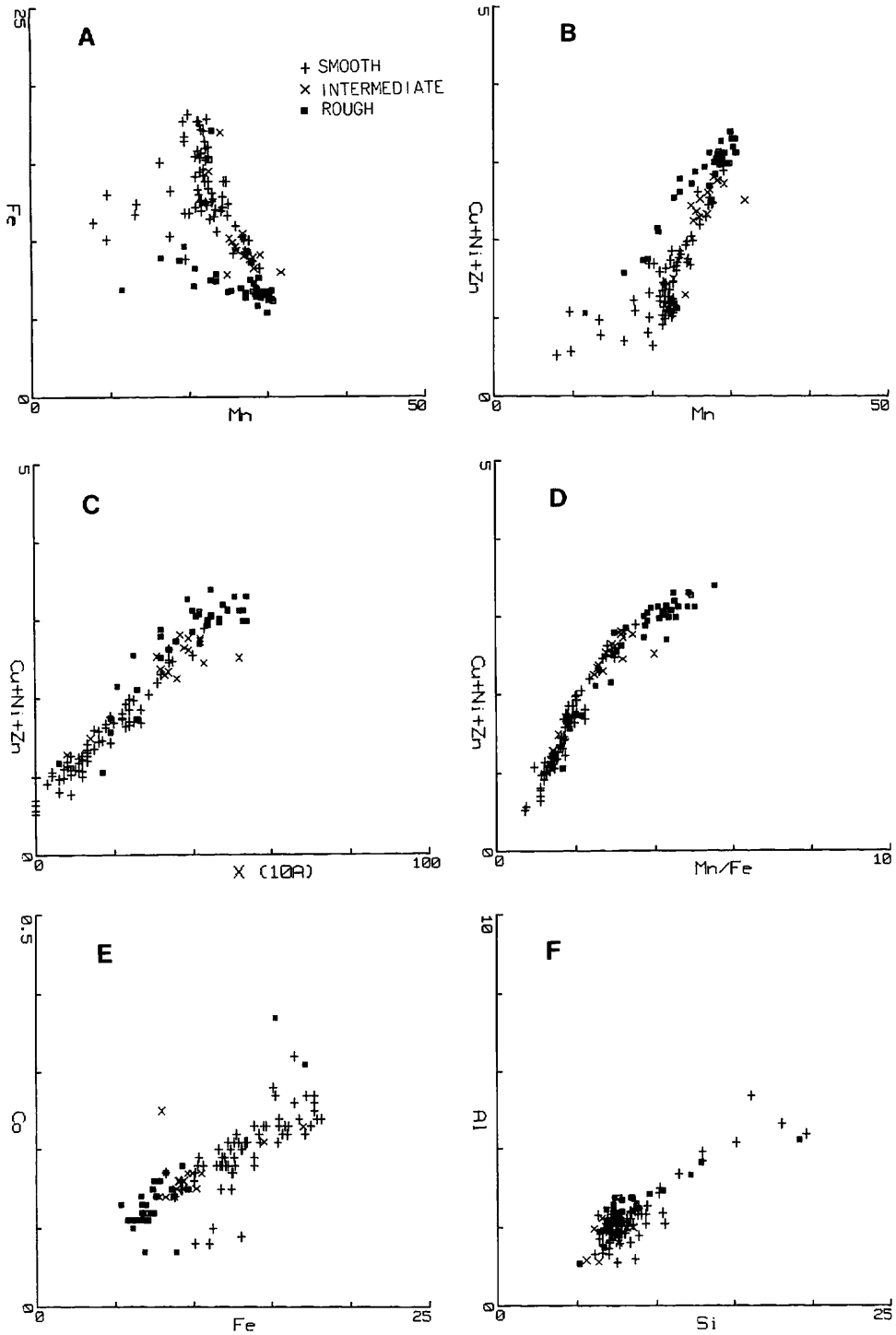

Fig. XII-2 Correlation plots of chemical and mineral composition. Three morphological types (smooth, rough, intermediate) are merged into a slightly scattered line in most of the diagrams.

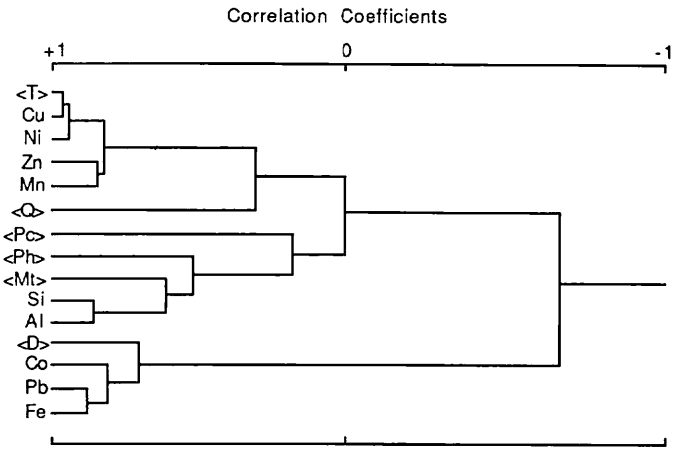

Fig. XII-3 Cluster analysis of chemical and mineral composition, showing three distinct groups related to the buserite, vernadite, and aluminosilicate phases. The new coefficients were calculated by simple arithmetical averaging from two coefficients between components or groups.
T: buserite, Q: quartz, Pc: plagioclase, Ph: phillipsite, Mt: montmorillonite, D: vernadite.

high concentrations of Mn and low Fe for type-r nodules are reflected by high contents of buserite, whereas high Fe and low Mn reflected by high contents of vernadite.

The small-scale variation in chemical composition of nodules is illustrated as polygons combined with nodule morphological types in Figure XII-5. Variation of the ratio Mn/Fe agrees generally with nodule type. The ratio and total Cu+Ni+Zn for type-s nodules is always low. The area covered with horizontally elongated symbols matches the area of thin or scarce development of uppermost transparent layers on SBP records. These areas generally match topographic highs and steep scarps. In contrast, type-r nodules always represent high Mn/Fe ratio and Cu+Ni+Zn mainly in basin areas. As mentioned in the previous section, this relationship is primarily determined by preferential deposition of manganese minerals controlled by sedimentary condition.

Polished cross sections of nodules from each station were stratigraphically examined under reflecting microscope according to our earlier mineralogical criteria (Usui, 1979a). Conformable and unconformable boundaries between the phases are frequently observed within nodules. The boundaries that can be compared to sedimentary hiatus, suggest sequential growth and breakup of nodules. Typical stratigraphy of nodules is shown as cross sections in Figure XII-6, and summarized as follows. Patterns of growth sequence are categorized as follows: Stratigraphical types (A):nodules entirely composed of laminated texture of buserite, showing continuous deposition, (B):nodules entirely composed of vernadite, commonly with hiatus, (C):nodules with the youngest vernadite layers surrounding internal older buserite layers, and other more complicated sequences in some nodules. Local variation of the internal nodule sequences in the detailed survey area is shown in Figure XII-7 together with thickness of the acoustic transparent layers. Notable is that the areal distribution of the sequence types are well correlated with distribution of transparent layers and topography. The

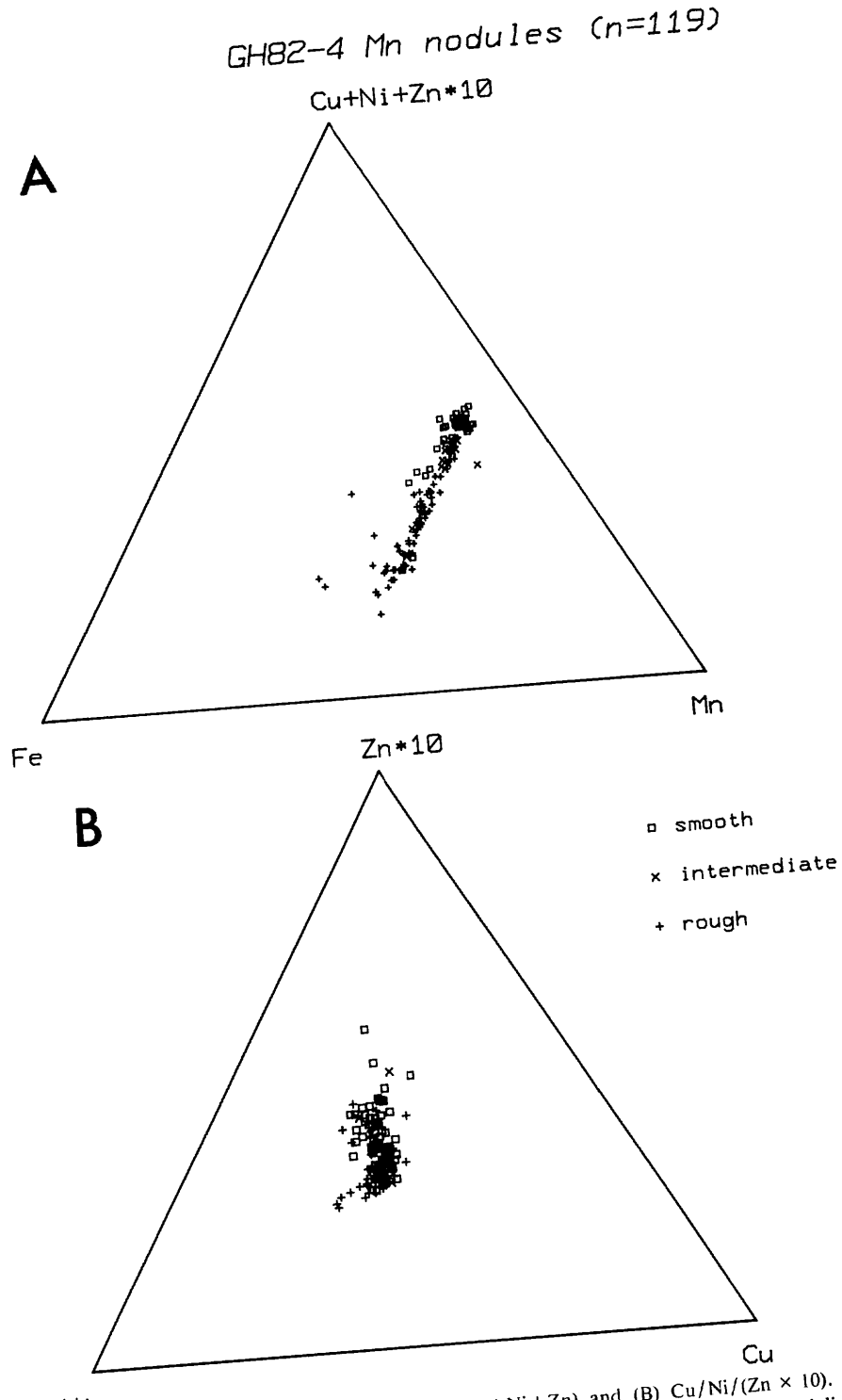

Fig. XII-4 Ternary diagram of ratios, (A) Fe/Mn/(Cu+Ni+Zn) and (B) Cu/Ni/(Zn × 10). Total Cu+Ni+Zn is linearly dependent of Mn and Fe contents, and the extrapolated line encounters the compositions of ideal buserite and vernadite on triangle axes.

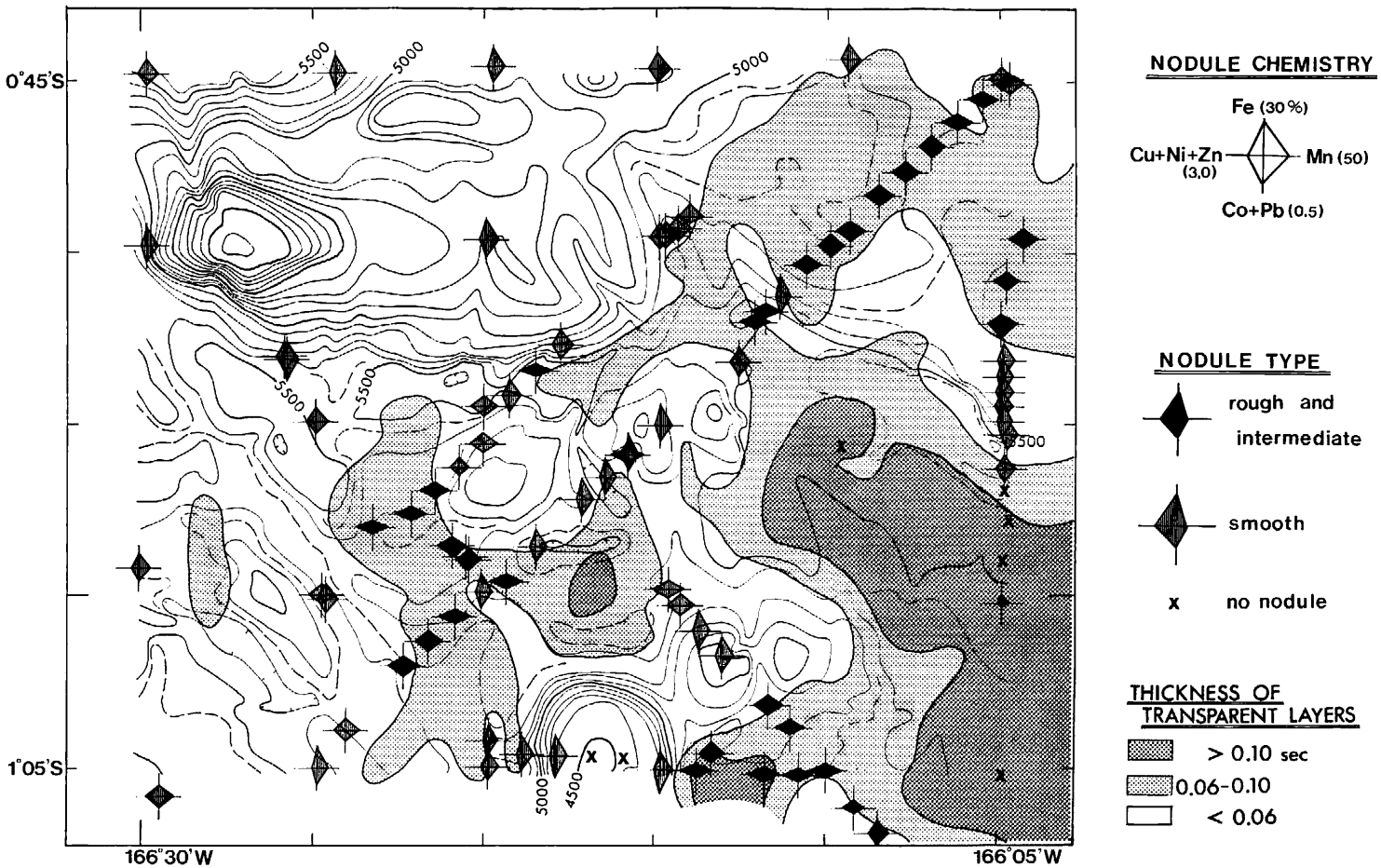

Fig. XII-5 Local small-scale variation of nodule chemical compositions within the detailed survey area. Horizontally elongated symbols (high Mn/Fe and high Cu+Ni+Zn) are closely associated with rough-surface nodules and also areas of moderate development of transparent layers.

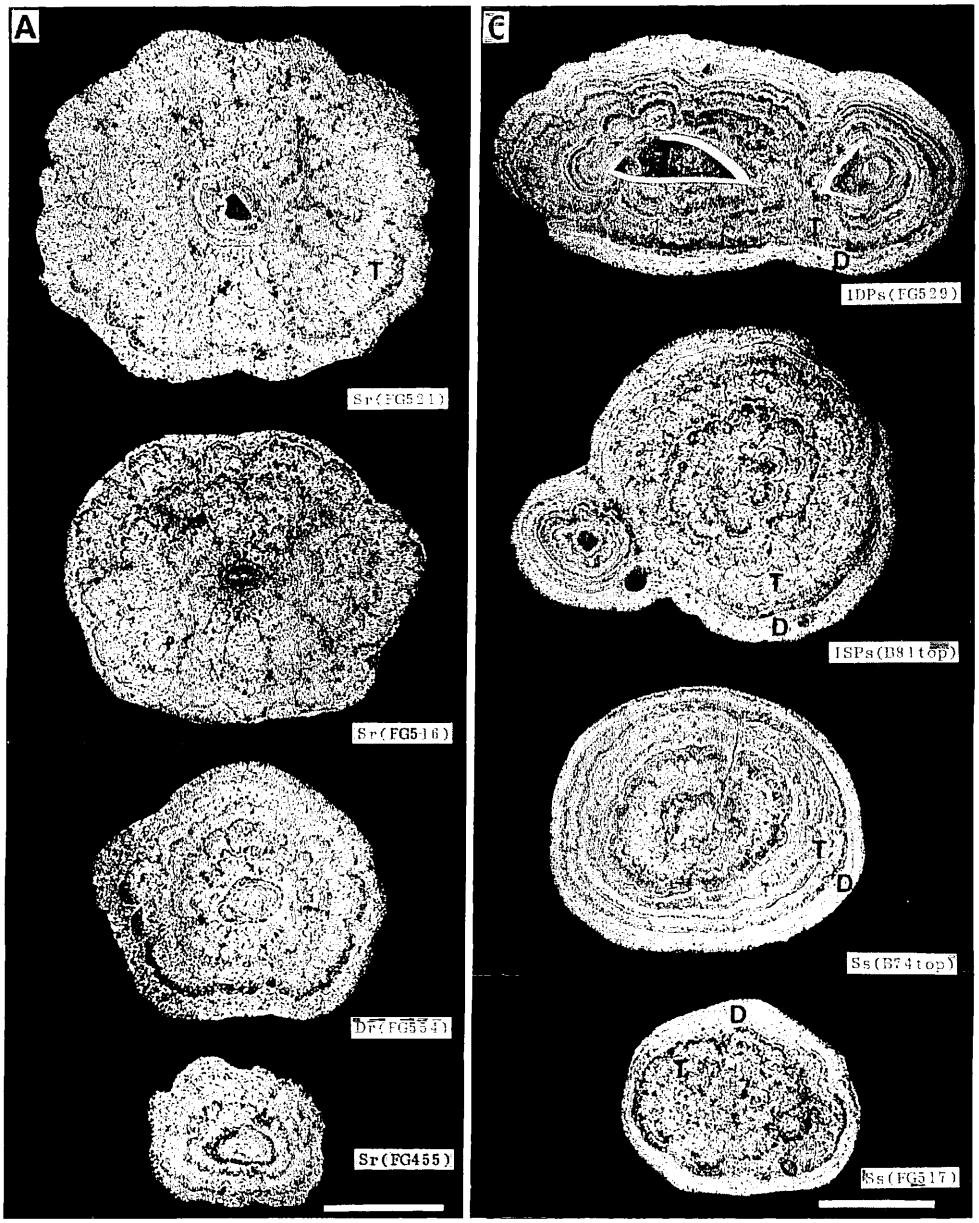

Fig. XII-6 Photographs of cross sections of manganese nodules under reflecting lights, showing typical internal mineralogical sequence in nodules. Scale bar:1 cm. Morphological type; I=irregular, S=spheroidal, D=discoidal, P=polynucleated, s=smooth, r=rough. Sequences (A) diagenetic nodules consisting completely of buserite (T in photos). (B) hydrogenous nodules consisting completely of vernadite, (D in photos), *left three* continuous lamination without growth hiatus, *right three* two growth stages divided by a marked growth hiatus. (C) nodules with two growth stages; the younger vernadite layers surrounding the older buserite nodule. (D) complicated growth structures of large nodules, reflecting several changes of forming conditions during growth.

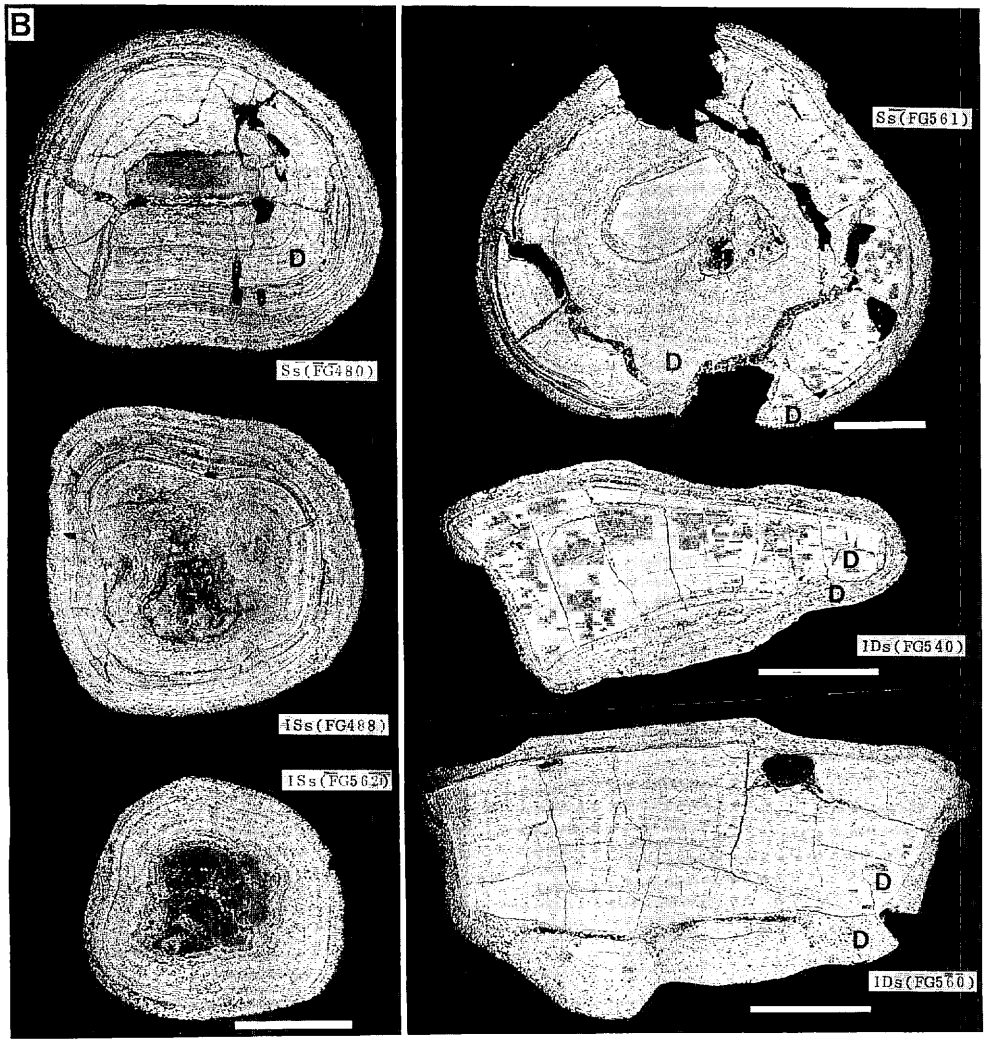

Fig. XII-6 (continued)

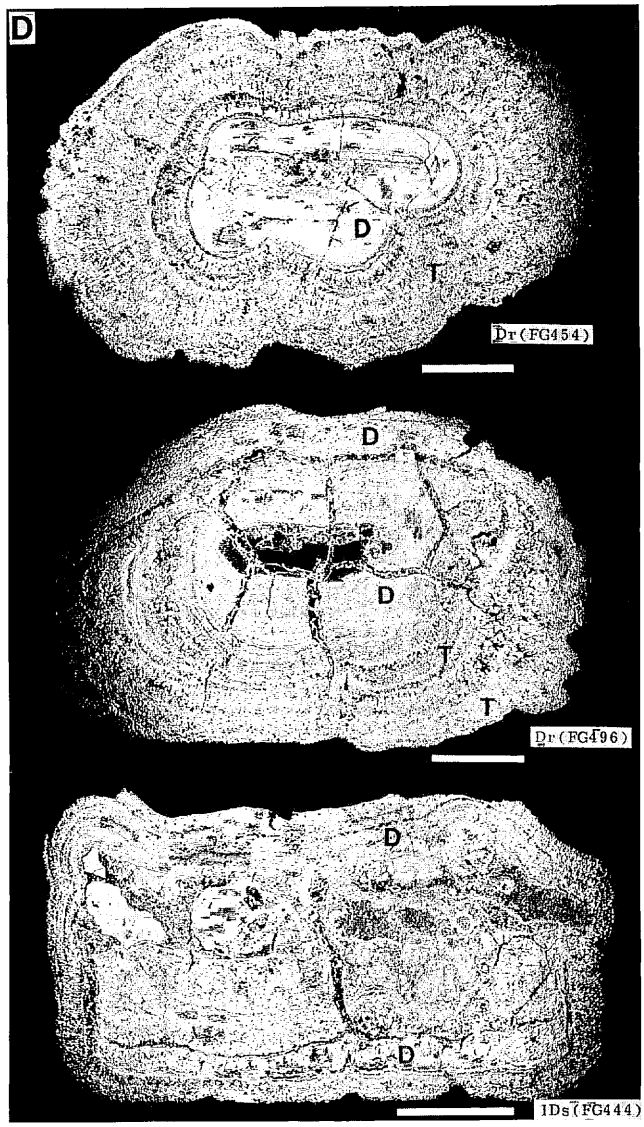

Fig. XII-6 (continued)

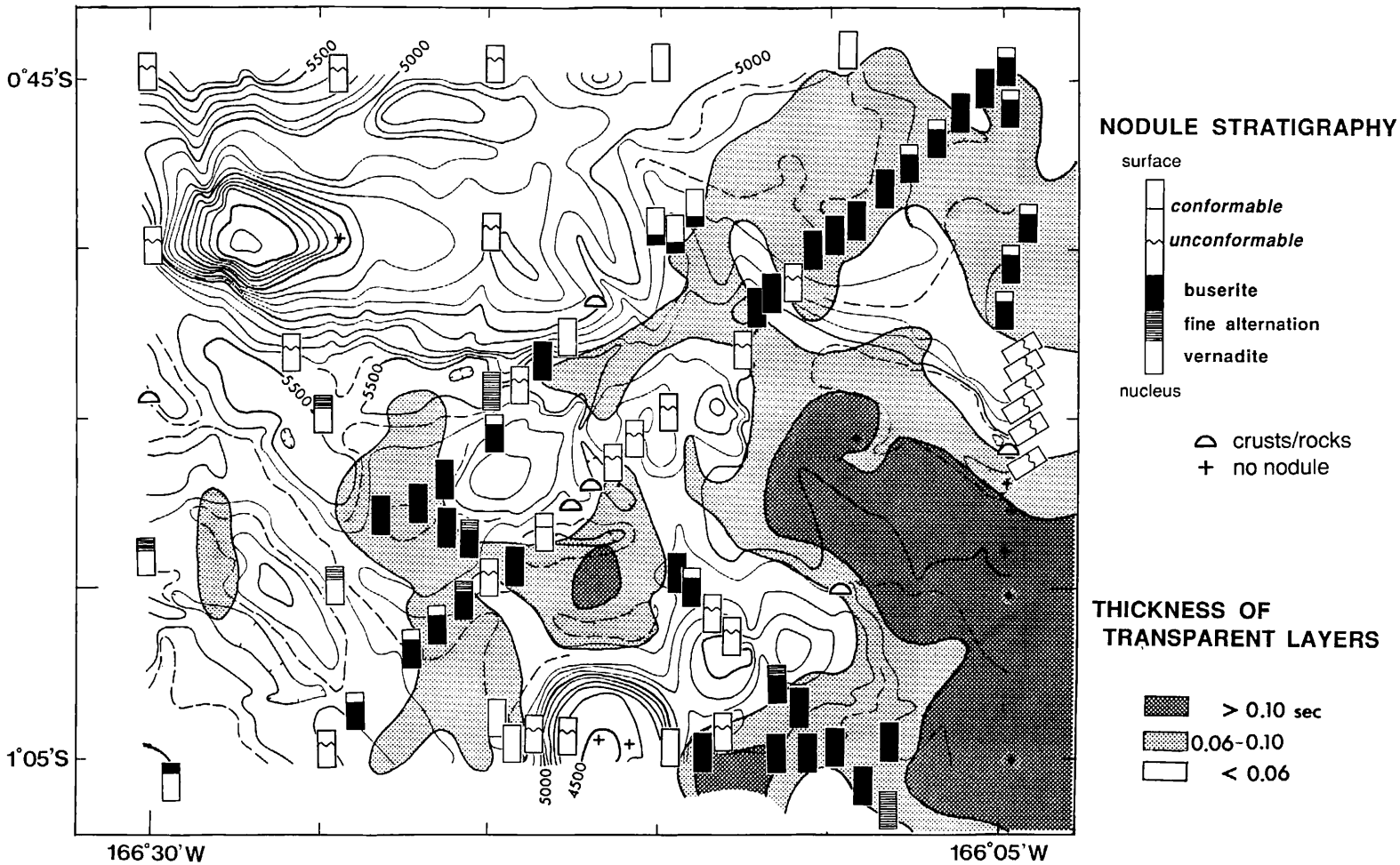

Fig. XII-7 Local variation of internal mineralogical sequence in nodules, showing a close relationship of buserite development with diagenetic condition caused by moderate and continuous sedimentation, and in contrast a relationship of vernadite with apparent outcrops of the older substrata.

sequence A develops in the basin area of moderate development of transparent layers (0.06–0.10 seconds in thickness), although thicker transparent layers yield no nodules in the eastern basin. The sequence B develops in the nodules of northeastern terrace area together with sequence A. The sequence C preferentially develops in the area with thin or scarce transparent layers, e.g., northern to western seamount area, an isolated seamount in the southern end, and scarp slope in the west. These variation of nodule stratigraphy suggests a quite local change of sedimentary condition in space and time, such as induced by bottom currents. The other complicated sequences are encountered near the areal boundaries of nodule morphological type.

The internal structure of the nodules are well related with development of uppermost transparent layers in the detailed survey area, though more precise age data of nodules are needed to correlate each sequence with local sedimentary history. This study points out a possibility of nodule stratigraphy as records of change in sedimentary condition, when it is described on mineralogical and microstructural criteria.

Characteristics of buried manganese nodules in sediment cores

Some manganese nodules occur within sediments in the five piston cores (max. depth 8 meters) and four box cores (max. depth 50 cm) among 20 piston and 14 box cores in the GH82-4 area. These nodules are found buried at depths of around 0.1 to 7 meters below the sea floor. The buried nodules are similar to the sea-floor nodules in shape, surface feature, chemistry, and mineralogy, although their size appear smaller ranging from several to 20 mm in diameter. The shape is variable from spherical to polynucleated discoidal; the surfaces are smooth and rough; constituent manganese minerals are buserite and/or vernadite. Silicate minerals are commonly incorporated. The ranges of compositional variation is 1.7 to 6.1 for ratio Mn/Fe, 1.5 to 3.1 wt.% for total Cu+Ni+Zn, 6.2 to 10.2 for Si content; all of which are within the range of sea-floor nodules (Table XII-4). Inter-element correlations are also similar.

As discussed in chapter VI (Nishimura and Ikehara, this volume), most of the nodules are within the Quaternary siliceous clay sediments above the Plio-Pleistocene hiatus (box cores and piston cores P349, P350), and few of them are within the Miocene siliceous ooze sediments below the hiatus (P342). These "fossil" nodules may have ceased growing, being prevented by temporary rapid sedimentation.

Table XII-1 Chemical and mineral composition of sea-floor manganese nodules.

n	Sta./	Sample no.	Tp	Mineral composition						Chemical composition (wt.%)											Analyzed number and part	
				T10	D	Qz	Ph	Pc	Mt	Mn	Fe	Cu	Ni	Co	Pb	Zn	Si	Al	H_2O+	H_2O-*		
1	3247	FG425	S	X	-	X	-	X	-	24.55	13.87	0.75	0.91	0.18	0.079	0.086	7.38	1.78	10.22	20.26	1/2	entire
2	3248	FG426-1	S	X	X	X	X	X	-	22.99	12.57	0.71	0.80	0.21	0.061	0.086	9.35	2.08	9.73	19.58	frag.	inside
3	3248	FG426-2	S	X	-	+	-	X	-	22.27	15.18	0.49	0.65	0.27	0.090	0.074	7.60	1.79	10.68	20.62	1	entire
4	3249	FG427	S	X	-	+	-	X	-	20.20	11.85	0.72	0.88	0.19	0.057	0.085	10.51	2.08	11.47	14.27	1	entire
5	3251	FG428	S	X	-	X	X	X	-	20.96	12.23	0.69	0.82	0.21	0.061	0.079	10.42	2.37	9.22	19.20	1/2	entire
6	3253	FG430	S	-	-	X	XX	-	X	7.89	11.21	0.21	0.27	0.10	0.041	0.036	19.64	4.36	11.17	12.23	1	entire
7	3254	FG431	S	-	X	X	-	-	-	19.62	16.43	0.48	0.44	0.32	0.086	0.082	8.66	1.20	10.64	21.57	2	entire
8	3258	FG435	S	-	X	X	-	X	-	16.37	15.05	0.29	0.36	0.28	0.073	0.054	8.93	1.78	9.01	20.35	1/2	entire
9	3260	FG437	R	XX	-	XX	-	X	-	23.46	7.41	0.89	1.63	0.15	0.022	0.092	9.60	2.84	12.50	11.13	1	entire
10	3262	P 337top	I	X	-	X	-	-	-	22.69	14.48	0.58	0.83	0.21	0.065	0.085	7.66	1.59	10.22	21.46	1	entire
11	3265	FG442	R	XX	X	XXX	-	X	-	20.80	8.25	0.71	1.25	0.17	0.010	0.147	-	3.40	-	9.82	1	entire
12	3267	FG444	S	+	-	+	XX	X	X	13.23	11.74	0.36	0.55	0.15	0.033	0.060	15.10	4.15	8.80	16.11	1/2	entire
13	3268	FG445	S	X	-	+	XX	X	-	23.24	12.73	0.70	0.92	0.22	0.053	0.088	8.14	2.13	10.28	19.56	1	entire
14	3274	FG451	R	X	-	XX	+	X	-	16.43	8.88	0.59	0.92	0.07	0.053	0.060	12.89	3.66	9.30	11.78	1	entire
15	3275	FG452	S	+	-	-	-	-	-	21.39	17.67	0.41	0.65	0.26	0.070	0.077	6.64	1.34	10.94	23.51	1	entire
16	3276	FG453	S	X	-	XX	X	X	X	9.51	10.07	0.38	0.64	0.08	0.010	0.052	18.08	4.64	9.18	8.04	2	entire
17	3277	FG454	R	XXX	-	X	-	-	X	28.64	6.76	1.26	1.67	0.12	0.017	0.131	6.93	2.03	9.08	16.75	3	entire
18	3278	FG455	R	XX	-	X	-	X	-	28.56	6.43	1.21	1.73	0.11	0.016	0.135	6.41	1.88	12.58	12.29	1	entire
19	3279	FG456	R	XX	-	XX	-	X	-	23.48	7.83	1.14	1.55	0.16	0.020	0.100	8.92	2.48	11.42	11.97	1	entire
20	3280	FG457	R	XX	-	XX	-	X	-	25.44	6.77	1.03	1.74	0.12	0.010	0.105	8.72	2.53	11.23	13.76	2	entire
21	3282	FG459	S	X	-	X	XX	X	-	13.48	12.42	0.31	0.41	0.15	0.039	0.046	12.97	3.67	9.61	18.17	1/2	entire
22	3283	FG460	R	XX	-	X	-	X	-	27.23	6.33	1.15	1.44	0.11	0.020	0.109	7.88	2.70	10.87	12.46	1/2	entire
23	3283	B 73	R	XX	-	XX	-	X	-	25.01	6.71	0.91	1.72	0.13	0.027	0.091	8.46	2.74	12.85	11.91	1	entire
24	3284	FG461	S	X	-	X	XX	X	-	17.69	10.31	0.50	0.66	0.19	0.036	0.064	12.93	3.93	9.09	20.23	1/2	entire
25	3287	FG464	S	+	X	+	-	X	-	19.43	17.64	0.32	0.42	0.27	0.065	0.056	7.64	1.95	10.03	23.28	1/2	entire
26	3295	FG472	R	XXX	-	XX	-	X	-	30.51	6.29	1.32	1.66	0.11	0.011	0.134	7.01	2.06	8.49	16.85	1/2	entire
27	3297	FG474	R	XXX	-	X	-	X	-	30.52	6.81	1.29	1.88	0.12	0.012	0.127	6.97	2.04	8.32	19.72	1/2	entire
28	3299	FG476	I	XX	-	XX	-	X	-	27.84	8.80	1.19	1.50	0.14	0.027	0.112	7.60	2.25	9.22	20.00	2	entire
29	3300	FG477	S	X	X	X	-	X	-	25.16	12.43	0.85	1.04	0.17	0.028	0.092	7.18	1.84	9.77	20.86	1/2	entire
30	3300	B 74/top	S	XX	-	X	-	-	-	25.00	11.67	0.86	1.10	0.18	0.034	0.096	7.21	1.80	10.67	19.87	1/2	entire
31	3300	B 74/bur.?	S	XX	-	+	-	-	-	24.44	12.21	0.84	1.04	0.18	0.031	0.091	8.00	1.85	10.13	19.66	1	entire
32	3301	FG478	R	X	-	XXX	-	X	-	11.43	6.89	0.41	0.60	0.07	0.010	0.046	19.19	4.23	10.51	9.47	1	entire
33	3303	FG480	S	X	X	X	-	-	-	20.98	14.11	0.50	0.71	0.22	0.051	0.065	8.11	2.20	8.83	21.71	1/2	entire
34	3304	FG481	S	X	-	XX	-	-	-	23.45	12.05	0.81	0.96	0.18	0.030	0.083	8.47	2.36	11.49	21.05	1/2	entire
35	3306	FG483	S	X	X	X	-	-	-	20.97	15.42	0.50	0.64	0.23	0.058	0.070	8.06	1.84	11.10	21.26	1	entire
36	3307	FG484	S	X	-	X	X	X	-	22.33	12.47	0.71	0.95	0.17	0.039	0.071	8.70	2.41	10.52	21.25	1	entire
37	3308	FG485	S	+	X	+	-	-	-	21.50	15.36	0.50	0.62	0.21	0.063	0.067	7.83	1.84	10.74	22.32	1	entire
38	3310	FG487	S	X	-	XX	X	-	-	21.66	12.62	0.57	0.79	0.18	0.044	0.075	9.41	2.55	10.37	20.20	1	entire
39	3311	FG488	S	+	-	-	-	-	-	21.50	17.45	0.37	0.54	0.23	0.072	0.067	7.11	1.60	11.66	23.30	1	entire
40	3312	FG489	S	X	-	X	-	X	-	22.97	13.13	0.66	0.92	0.20	0.041	0.082	7.86	2.12	10.73	21.78	1	entire
41	3312	P 341top	S	XX	-	X	-	-	-	25.78	9.18	1.08	1.45	0.15	0.016	0.096	8.18	2.16	9.56	19.38	1	entire
42	3313	FG490	S	X	-	+	XX	-	-	22.64	13.85	0.57	0.81	0.19	0.041	0.075	8.14	2.03	9.77	21.78	1	entire

Table XII-1 (continued)

n	Sta./	Sample no.	Tp	Mineral composition						Chemical composition (wt.%)											Analyzed number and part	
				T10	D	Qz	Ph	Pc	Mt	Mn	Fe	Cu	Ni	Co	Pb	Zn	Si	Al	H_2O+	H_2O-*		
43	3314	FG491	S	X	-	+	-	-	-	24.82	13.81	0.60	0.99	0.19	0.045	0.091	6.99	1.47	10.08	22.31	1	entire
44	3315	FG492	R	XX	-	X	-	X	-	28.03	8.56	1.13	1.61	0.15	0.028	0.108	7.34	2.22	9.21	18.39	3	entire
45	3316	FG493	I	+	X	+	-	-	-	24.15	16.94	0.46	0.75	0.23	0.063	0.082	6.38	1.11	10.83	22.49	1/2	entire
46	3317	FG494	I	XX	-	XX	-	X	-	27.06	9.02	1.11	1.39	0.16	0.017	0.108	8.18	1.99	9.35	17.33	1	entire
47	3318	FG495	S	X	X	+	-	-	-	21.94	17.07	0.37	0.60	0.22	0.059	0.121	7.05	1.31	10.48	13.36	1	entire
48	3320	FG496	I	XX	-	X	XX	-	-	25.23	10.17	1.00	1.16	0.15	0.023	0.094	8.51	2.00	9.52	20.63	1/4	entire
49	3321	FG497	R	XXX	-	X	-	X	-	28.94	7.59	1.31	1.62	0.14	0.012	0.116	7.32	2.27	8.79	18.69	4	entire
50	3322	FG498	R	XXX	-	X	-	-	-	30.26	6.68	1.35	1.72	0.12	0.011	0.126	7.06	1.91	9.47	17.60	1	entire
51	3323	FG499	S	X	-	X	-	X	-	21.42	13.03	0.59	0.79	0.20	0.038	0.074	9.04	2.33	10.40	20.98	1/2	entire
52	3324	B 75/top	R	XX	-	X	-	-	-	27.59	9.30	1.11	1.28	0.18	0.027	0.127	7.25	1.77	9.44	19.09	1/2	entire
53	3324	B 75/bur.	R	X	-	XX	XX	X	X	19.46	9.68	0.69	0.98	0.15	0.023	0.086	12.17	3.33	9.17	18.94	1/2	entire
54	3331	P 347top	I	XX	-	X	-	X	-	25.94	9.61	0.93	1.26	0.17	0.031	0.104	7.33	2.08	9.75	19.49	1	entire
55	3331	FG501	S	X	X	X	-	-	-	22.62	13.43	0.54	0.84	0.21	0.044	0.082	7.50	1.84	9.26	21.23	1/2	entire
56	3333	B 78	R	XX	X	XX	-	X	-	22.79	7.49	0.99	1.45	0.16	0.016	0.103	10.39	2.94	11.01	12.36	1	entire
57	3334	FG503	S	X	X	X	-	X	-	21.64	15.67	0.43	0.59	0.22	0.054	0.068	7.52	1.85	10.43	21.72	1	entire
58	3335	FG504	R	XXX	-	XX	-	-	-	30.06	6.17	1.28	1.88	0.11	0.014	0.129	7.47	2.37	9.15	16.13	1	entire
59	3336	FG505	S	XX	-	X	-	-	-	27.61	9.22	1.09	1.27	0.16	0.033	0.107	7.15	2.10	9.50	17.90	1	entire
60	3337	FG506	S	XXX	-	X	-	X	X	29.06	8.24	1.24	1.54	0.17	0.022	0.115	6.94	2.21	9.66	17.08	2	entire
61	3338	P 349top	S	XX	-	+	-	X	-	26.76	10.28	1.00	1.20	0.18	0.017	0.109	7.41	2.14	9.70	18.29	1	entire
62	3339	FG508	S	X	X	X	-	X	-	21.47	14.45	0.52	0.68	0.23	0.045	0.070	8.39	2.21	9.30	22.65	1	entire
63	3341	FG510	S	+	X	+	-	-	-	22.47	17.83	0.34	0.61	0.24	0.054	0.067	6.11	1.30	9.27	24.33	1/2	entire
64	3342	FG511	S	X	X	+	-	-	-	22.16	16.37	0.43	0.59	0.26	0.051	0.062	7.02	1.62	9.71	23.95	1	entire
65	3343	B 79/top	S	X	X	X	XX	-	-	19.62	11.83	0.53	0.72	0.18	0.036	0.067	10.17	2.88	9.96	19.87	1	entire
66	3343	B 79/burS	S	-	X	-	-	-	-	20.10	18.12	0.24	0.34	0.24	0.053	0.057	7.54	1.11	10.66	22.08	1	top
67	3343	B 79/burR	R	XXX	-	XX	-	-	-	29.90	5.40	1.15	2.13	0.13	0.023	0.109	7.61	1.96	8.78	22.47	1	bottom
68	3343	B 79bur.?I	S	XX	X	X	XX	-	-	22.37	12.31	0.75	1.03	0.20	0.038	0.075	8.64	2.45	9.37	18.25	1	inside
69	3344	FG512	I	XX	-	X	-	X	-	28.18	8.90	1.14	1.51	0.15	0.028	0.112	7.01	2.09	8.87	19.88	1	entire
70	3345	FG513	I	XX	-	X	-	X	-	27.34	9.33	1.10	1.43	0.15	0.022	0.108	6.91	2.07	9.25	19.91	1	entire
71	3346	FG514	I	XX	-	X	-	-	-	25.58	9.92	1.01	1.26	0.17	0.027	0.099	7.73	2.31	9.21	19.14	1	entire
72	3347	FG515	R	XX	-	XX	-	X	-	28.33	7.22	1.25	1.71	0.12	0.017	0.133	7.40	2.19	9.03	17.38	1	entire
73	3348	FG516	R	XXX	-	XX	-	X	-	28.62	6.93	1.21	1.64	0.13	0.017	0.122	7.47	2.32	9.58	18.78	2	entire
74	3349	P 350top	I	XX	X	X	-	-	-	26.03	9.37	1.01	1.41	0.16	0.024	0.109	7.65	2.21	9.08	23.35	1	entire
75	3349	FG517	I	XX	-	+	-	X	-	26.92	10.52	0.96	1.27	0.17	0.030	0.104	6.84	2.02	9.43	20.93	1	entire
76	3350	FG518	S	XX	-	X	-	-	-	27.12	10.13	1.05	1.24	0.17	0.029	0.160	6.84	1.90	9.55	21.38	1	entire
77	3351	FG519	I	XX	-	X	-	X	-	28.28	8.21	1.18	1.47	0.14	0.017	0.114	6.61	2.23	9.02	19.49	1	entire
78	3352	FG520	S	+	X	X	-	-	-	21.20	17.70	0.36	0.48	0.25	0.047	0.065	6.66	1.51	10.53	23.56	1	entire
79	3353	FG521	R	XXX	-	X	-	X	-	29.44	6.74	1.26	1.60	0.11	0.006	0.123	7.45	2.09	9.02	16.83	1	entire
80	3354	FG522	R	XXX	-	X	-	X	-	28.67	6.80	1.30	1.59	0.12	0.001	0.118	7.79	2.12	8.92	17.27	1/2	entire
81	3355	B 80/top	S	X	-	X	-	X	-	23.30	11.58	0.74	0.95	0.20	0.029	0.080	8.79	2.33	9.95	21.16	1/2	entire
82	3355	B 80/bur	S	X	X	X	X	X	-	21.26	13.30	0.58	0.70	0.21	0.046	0.069	8.50	2.05	9.92	22.15	1	entire
83	3356	FG523	R	X	-	XXX	-	X	-	20.59	7.13	0.69	1.33	0.11	0.000	0.127	-	3.21	-	10.36	1	entire
84	3357	FG524	S	X	X	X	XX	X	-	22.74	11.48	0.70	0.87	0.18	0.034	0.079	8.36	2.40	9.90	21.17	1/2	entire

Table XII-1 (continued)

n	Sta./	Sample no.	Tp	Mineral composition						Chemical composition (wt.%)											Analyzed number and part	
				T10	D	Qz	Ph	Pc	Mt	Mn	Fe	Cu	Ni	Co	Pb	Zn	Si	Al	H_2O+	H_2O-*		
85	3358	FG525	S	X	-	X	-	X	X	23.68	10.63	0.81	0.91	0.18	0.028	0.087	8.69	2.67	9.88	18.98	1	entire
86	3359	FG526	S	XX	-	XX	XX	-	-	19.64	8.80	0.70	0.92	0.14	0.026	0.076	11.47	3.35	9.59	17.71	1/3	entire
87	3360	FG527	R	XXX	-	X	-	X	-	29.74	6.54	1.21	1.65	0.11	0.022	0.118	7.03	2.19	9.41	17.94	2	entire
88	3361	FG528	R	XXX	-	X	-	X	-	27.84	7.45	1.24	1.62	0.12	0.007	0.132	7.83	2.39	9.31	16.95	2	entire
89	3362	FG529	I	XX	-	X	-	-	-	29.08	9.07	1.20	1.42	0.16	0.019	0.106	6.95	2.00	9.25	18.91	1	entire
90	3364	FG531	S	X	-	X	-	-	-	22.59	16.00	0.47	0.69	0.23	0.066	0.075	7.12	1.67	11.51	22.45	1	entire
91	3365	FG532	S	X	X	+	-	-	-	21.65	17.12	0.44	0.57	0.27	0.055	0.069	6.61	1.55	10.32	22.98	1	entire
92	3366	B 81	S	XX	-	X	XX	-	-	27.75	10.00	1.12	1.26	0.16	0.022	0.099	6.70	1.98	9.64	19.54	1	entire
93	3367	FG533	S	X	X	+	-	-	-	19.64	16.72	0.38	0.55	0.24	0.057	0.063	8.35	1.62	10.11	21.62	1	entire
94	3369	FG535	S	X	X	X	-	X	-	21.69	11.99	0.66	0.90	0.19	0.050	0.074	8.87	2.48	9.94	19.96	1	entire
95	3373	FG539	S	X	X	X	XX	-	-	21.52	12.59	0.57	0.77	0.19	0.044	0.075	9.37	2.33	10.04	20.42	1	entire
96	3374	FG540	S	X	-	X	-	-	-	21.96	14.22	0.45	0.75	0.21	0.051	0.075	7.60	1.72	10.12	21.45	1	entire
97	3375	FG541	S	X	X	+	XX	-	-	21.25	15.83	0.38	0.58	0.23	0.065	0.066	7.68	1.59	10.06	22.55	1	entire
98	3376	FG542	S	X	X	X	-	-	-	22.02	14.61	0.47	0.64	0.23	0.052	0.071	7.80	1.87	10.36	21.47	1	entire
99	3377	FG543	I	XXX	-	X	-	-	-	31.75	7.94	1.06	1.24	0.25	0.001	0.212	5.58	1.16	9.18	19.50	1	entire
100	3378	B 82	I	XXX	-	X	-	X	-	24.92	7.79	1.07	1.28	0.14	0.022	0.099	6.07	1.96	9.50	19.01	1	entire
101	3379	FG544	S	X	-	X	-	X	-	22.17	13.84	0.54	0.75	0.23	0.064	0.074	7.04	2.13	10.35	21.82	1	entire
102	3380	FG545	R	XXX	-	XX	-	X	-	30.73	6.11	1.46	1.51	0.10	0.006	0.141	7.12	2.04	8.83	16.59	1	entire
103	3381	FG546	S	XX	-	X	-	-	-	24.41	12.88	0.69	0.93	0.21	0.041	0.089	6.63	1.85	9.96	21.10	1/3	entire
104	3383	P 353top	S	XX	-	X	-	-	-	26.09	11.03	0.98	1.12	0.08	0.032	0.102	7.25	2.23	9.20	17.49	1/2	entire
105	3383	FG548	S	X	X	X	-	-	X	24.27	11.95	0.81	1.03	0.19	0.033	0.088	7.15	2.34	9.35	19.51	1	entire
106	3384	FG549	S	XX	-	X	-	X	-	27.20	9.27	1.12	1.31	0.15	0.019	0.112	6.33	2.30	8.99	18.95	1	entire
107	3385	FG550	R	XX	-	XXX	-	X	-	18.78	8.73	0.60	1.04	0.14	0.005	0.093	-	3.70	-	12.08	1	entire
108	3386	FG551	R	XXX	-	XX	-	X	-	26.71	6.97	1.16	1.67	0.12	0.017	0.106	7.68	2.76	9.03	14.68	1	entire
109	3387	FG552	R	XXX	-	X	-	X	-	28.47	6.59	1.30	1.71	0.11	0.007	0.119	7.35	2.55	8.85	15.70	1	entire
110	3388	B 83	R	XX	-	X	-	X	-	28.75	5.84	1.33	1.81	0.11	0.015	0.131	7.33	2.58	8.97	15.49	2	entire
111	3389	FG553	R	+	-	+	-	-	-	22.68	15.18	0.55	0.55	0.37	0.058	0.074	6.70	1.49	10.39	22.49	1/2	entire
112	3390	FG554	R	XX	-	XX	-	X	-	28.17	6.68	1.29	1.64	0.12	0.011	0.113	7.31	2.52	9.06	16.92	2	entire
113	3392	FG556	R	XX	-	XX	-	-	-	27.20	6.65	1.21	1.79	0.14	0.011	0.108	7.39	2.75	9.08	16.42	2	entire
114	3393	FG557	R	XXX	-	XX	-	X	-	29.16	6.31	1.33	1.67	0.11	0.011	0.121	6.89	2.45	8.71	17.49	1/2	entire
115	3397	FG560	R	X	X	-	-	-	-	23.10	17.08	0.44	0.60	0.31	0.073	0.074	5.15	1.06	10.71	22.76	1/3	entire
116	3398	FG561	S	+	X	X	-	X	-	22.56	15.41	0.41	0.58	0.24	0.054	0.063	6.78	1.96	10.47	22.92	1	entire
117	3399	B 84/top	S	-	-	+	-	X	X	9.64	13.00	0.23	0.29	0.09	0.015	0.039	16.13	5.37	7.65	12.85	2	entire
118	3399	B 84/bur	S	X	-	XX	XX	X	X	17.77	13.21	0.43	0.59	0.21	0.040	0.062	10.28	2.99	9.90	20.15	1	entire
119	3402	FG562	S	+	X	-	-	-	-	22.34	15.94	0.38	0.65	0.22	0.061	0.072	6.45	1.71	10.00	23.37	1	entire

Note: Tp /type of nodule (S: smooth surface, R: rough surface, I: intermidiate)
Mineralogy / T10: 10 Å manganate, D: δ-MnO_2(calculated), Qz: quartz, Ph: phillipsite, Pc: plagioclase, Mt; montmorillonite.
Mineral compositions are presented as relative abundance; comparison between minerals is not available.
XXX: very abundant, XX: abundant, X: common, +: traceable, -: not detected.
All concentrations normalized to 110°C dried samples; except for *H_2O- to air dried samples.

Table XII-2 Summary of chemical composition of three types of manganese nodiles.

Morphological type	smooth		intermediate		rough		total			
Number of samples	67		15		37		119			
Elements	AV	SD	AV	SD	AV	SD	AV	SD	Max	Min
Mn	21.65	±3.98	26.73	±2.20	26.10	±4.47	23.67	±4.57	31.75	7.89
Cu	0.60	±0.24	1.00	±0.21	1.07	±0.29	0.80	±0.34	1.46	0.21
Ni	0.79	±0.27	1.28	±0.23	1.50	±0.37	1.07	±0.45	2.13	0.27
Zn	0.078	±0.020	0.110	±0.030	0.112	±0.023	0.092	±0.027	0.212	0.037
Fe	13.34	±2.52	10.00	±2.48	7.60	±2.29	11.14	±3.57	18.12	5.4
Co	0.200	±0.045	0.170	±0.034	0.136	±0.055	0.176	±0.055	0.37	0.07
Pb	0.046	±0.017	0.028	±0.017	0.018	±0.015	0.035	±0.021	0.090	-0.001
*Si	8.64	±2.62	7.13	±0.79	8.16	±2.46	8.31	±2.45	19.64	5.15
Al	2.22	±0.81	1.94	±0.37	2.48	±0.63	2.26	±0.73	5.37	1.06
*H_2O^+	10.01	±0.73	9.45	±0.50	9.74	±1.22	9.86	±0.89	12.85	7.65
#H_2O^-	20.2	±2.9	20.1	±1.5	15.9	±3.5	18.8	±3.6	24.3	8.0
Mn/Fe	1.70	±0.55	2.81	±0.66	3.67	±1.08	2.45	±1.18	5.54	0.70
Cu+Ni+Zn	1.47	±0.53	2.39	±0.44	2.69	±0.65	1.96	±0.80	3.39	0.52

Analyses made on 110°C dried basis except for water content (#H_2O^-).

Ave:average, SD:one standard deviation, Max:maximum, Min:minimum, H_2O^+:loss of ignition.

*:three data (nos. 11, 83, 107, r-type nodules) are omitted.

Table XII-3 Matrix of correlation coefficients between mineral and chemical composition.

	tm	Cu	Ni	Zn	Mn	qtz	pc	ph	mt	Si	Al	dm	Co	Pb	Fe
*tm	1														
Cu	0.96	1													
Ni	0.94	0.95	1												
Zn	0.85	0.85	0.80	1											
Mn	0.82	0.85	0.81	0.86	1										
*qtz	0.44	0.42	0.47	0.23	0.11	1									
*pc	0.10	0.06	0.09	-0.08	-0.24	0.29	1								
*ph	-0.26	-0.30	-0.31	-0.36	-0.50	0.01	-0.03	1							
*mt	-0.22	-0.24	-0.24	-0.28	-0.51	-0.03	-0.24	0.49	1						
Si	-0.34	-0.38	-0.34	-0.50	-0.78	0.32	0.47	0.58	0.65	1					
Al	-0.02	-0.05	-0.01	-0.28	-0.51	0.46	0.62	0.50	0.57	0.86	1				
*dm	-0.80	-0.77	-0.74	-0.66	-0.55	-0.31	-0.21	0.05	-0.03	0.06	-0.20	1			
Co	-0.65	-0.62	-0.65	-0.38	-0.23	-0.57	-0.47	-0.10	-0.24	-0.33	-0.59	0.67	1		
Pb	-0.79	-0.76	-0.75	-0.61	-0.46	-0.55	-0.29	0.03	-0.09	-0.08	-0.39	0.71	0.78	1	
Fe	-0.88	-0.86	-0.88	-0.67	-0.53	-0.65	-0.31	0.03	-0.02	-0.07	-0.38	0.79	0.82	0.87	1

Mineral components are marked with *. tm:10Å manganate, dm:δ-MnO_2, qtz:quartz, pc:plagioclase, ph:phillipsite, mt:montmorillonites.

Table XII-4 Chemical and mineral composition of buried manganese nodules within sediment cores.

Sta./	Sample no.	Depth from top (cm)	Tp	Mineral composition						Chemical composition (wt.%)											Analyzed number and part	
				T10	D	Qz	Ph	Pc	Mt	Mn	Fe	Cu	Ni	Co	Pb	Zn	Si	Al	H_2O+	H_2O-*		
3315	P342-VII59	637	I	XXX	X	+	-	-	-	27.84	6.80	1.19	1.31	0.21	0.014	0.092	8.53	1.90	10.55	11.16	1	entire
3315	P342-VIII90	768	R	XXX	X	XX	-	X	-	26.43	5.55	1.09	1.59	0.16	0.015	0.093	10.16	3.04	8.69	13.30	1	entire
3315	P342-V87	465	I	XXX	X	X	-	X	-	30.56	6.55	1.44	1.53	0.15	0.014	0.110	6.93	2.14	8.83	16.21	1	entire
3349	P350-III40	172	I	XX	X	X	XX	X	X	23.38	8.90	0.94	1.32	0.17	0.021	0.095	8.56	3.02	10.55	15.35	1	entire
3383	P353-VI60	535	R	XXX	X	XX	-	-	-	30.60	5.02	1.06	2.04	0.13	0.018	0.118	7.29	2.32	8.47	14.81	1	entire
3383	P353-III	11	S	X	X	X	-	-	-	23.76	11.85	0.78	1.02	0.19	0.034	0.086	7.93	2.53	9.51	20.16	1/2	entire
3400	P355-VIII50	80	S	X	X	+	-	-	-	20.69	11.85	0.74	0.75	0.23	0.044	0.078	9.63	2.87	13.85	11.10	1	entire
3400	P355-I80	715	R	XX	X	X	-	-	-	28.28	8.93	1.14	1.41	0.19	0.028	0.107	6.16	2.02	9.19	19.49	1/2	entire

Notes are common to Table 1.

References

Andrews, J. E. and Friedrich, H. W. (1979) Distribution patterns of manganese nodule deposits in the Northeast Equatorial Pacific. *Marine Mining*, vol. 2, p. 1–44.

Boles, J. R. (1977) Zeolites in deep-sea sediments. In: F.A. Mumpton (ed.) Mineralogy and Geology of Natural Zeolites. *Mineral. Soc. Am. Short Course Notes*, vol. 4, p. 137–163.

Bonatti, E., Honnorez, J., Joensuu, O. and Rydell, H. (1972) Classification and genesis of submarine iron-manganese deposits. In: D. R. Horn (ed.) *Ferromanganese Deposits on the Ocean Floor*. N.S.F., Washington D.C., p. 149–166.

Burns, R. G. and Burns, V. M. (1977) Mineralogy of Manganese Nodules. In: G.P. Glasby (ed.) *Marine Manganese Deposits*. Elsevier Pub. Co. Ltd., p. 185–248.

———, Burns, V. M. and Stockman, H. W. (1983) A review of the todorokite-buserite problem: implication to the mineralogy of marine manganese nodules. *Amer. Mineral.*, vol. 68, p. 972–980.

Cronan, D. S. (1980) *Under Water Minerals*. Academic Press, London. , p. 1–362.

——— (1986) *Sedimentation and Mineral Deposits in the Southwestern Pacific Ocean*. Acad. Press, London, p. 1–344.

Exon, N. F. (1983) Manganese nodule deposits in the Central Pacific Ocean and their variation with latitude. *Mar. Mining*, vol. 4, no. 1, p. 79–107.

Frazer, J. L. and Fisk, M. B. (1981) Geological factors related to characteristics of sea-floor manganese nodule deposits. *Deep-Sea Res.*, vol. 28A, no. 12, p. 1533–1551.

Giovanoli, R. (1980) On natural and synthetic manganese nodules. In: Varentsov, I. (ed.) *Geology and Geochemistry of Manganese*, vol. 1, Hungarian Acad. Sci. Publ., p. 159–202.

Glasby, G. P., Meylan, M. A., Margolis, S. V. and Backer, H. (1980) *Manganese deposits of the Southwestern Pacific Basin*. In: I. M. Varentsov and G. Y. Grasselly (eds.) *Geology and Geochemistry of Manganese*, vol. III, Hungar. Acad. Sci., Budapest, p. 137–183.

Halbach, P. and Özkara, M. (1979) Morphological and geochemical classification of deep-sea ferromanganese nodules and its genetical interpretation. In: C. Lalou (ed.), *La Genèse des Nodules de Manganèse*, Colloques Internationaux du C.N.R.S., no. 289, p. 77–89.

———, Özkara, M. and Hence, J. (1975) The influence of metal content of the physical and mineralogical properties of pelagic manganese nodules. *Mineral. Deposita*, vol. 10, p. 397–411.

Hein, P. (1977) Geochemie des nodules de pacifique nord-est etude statistique. *Sci. Tech. Rept.* C.N.E.X.O., no. 35, p. 1–74.

Mckelvy, V. E. (1986) Subsea Mineral Resources. *U.S. Geol. Surv. Bull.*, no. 1689–A, p. 1–106.

Mizuno, A., Miyazaki, T., Nishimura, A., Tamaki, K. and Tanahashi, M. (1980) Central Pacific manganese nodules, and their relation to sedimentary history. In: *Proc. 12th Ann. Offshore Tech. Conf.*, vol. 3, Houston, p. 331-340.

——— and Nakao, S. (1982) Regional Data of Marine Geology, Geophysics, and Manganese Nodules: The Wake-Tahiti Transect in the Central Pacific. *Geol. Surv. Japan Cruise Rept.*, no. 18, p. 1-399.

Mochizuki, T. and Terashima, S. (1983) Chemical analysis of manganese nodules. *Methods of Chemical Analysis in G.S.J.*, no. 53, p. 1-36.

Ostwald, J. (1984) Ferruginous vernadite in an Indian Ocean ferromanganese nodule. *Geol. Mag.*, vol. 121, no. 5, p. 483-488.

Piper, D. Z., Cannon, W. and Leong, K. (1977) Composition and abundance of ferromanganese nodules at DOMES sites A, B and C: relationship with bathymetry and stratigraphy. In: D.Z. Piper (ed.) *Deep Ocean Environmental Study: Geology and Geochemistry of DOMES Sites A, B and C, Equatorial North Pacific*, p. 217-266.

Sorem, R. K., Reinhart, R. H., Fewks, R. H. and McFarland W. D. (1979) Occurrence and character of manganese nodules in DOMES Sites A, B, and C, East Equatorial Pacific Ocean. In: J. L. Bischoff and D. Z. Piper (eds.) *Marine Geology and Oceanography of the Pacific Manganese Nodule Province*, Mar. Sci. Ser., Plenum Pub. Co., p. 475-527.

Terashima, S. (1978) Atomic absorption analysis of Mn, Fe, Cu, Ni, Co, Pb, Zn, Si, Al, Ca, Mg, Na, K, Ti, and Sr in manganese nodules. *Bull. Geol. Surv. Japan*, vol. 29, p. 401-411.

Usui, A. (1979a) Minerals, metal contents, and mechanism of formation of manganese nodules from the Central Pacific Basin (GH76-1 and GH77-1 areas). In: Bischoff, J. L. and Piper, D. Z. (eds.) *Marine Geology and Oceanography of the Pacific Manganese Nodule Provinces*, Plenum Pub. Co., p. 651-679.

——— (1979b) Nickel and copper accumulation as essential elements in 10 Å manganite of deep-sea manganese nodules. *Nature*, vol. 279, p. 411-413.

——— (1983) Regional variation of manganese nodule facies on the Wake-Tahiti Transect: morphological, chemical and mineralogical study. *Mar. Geol.*, vol. 54, p. 27-51.

———, Nishimura, A., Tanahashi, M. and Terashima, S. (1987) Local variability of manganese nodule facies on small abyssal hills of the Central Pacific Basin. *Mar. Geol.*, vol. 74, p. 237-275.

——— and Terashima, S. (1986) Local variability of manganese nodule chemistry around the small abyssal hills in the GH81-4 area. *Geol. Surv. Japan Cruise Rept.*, no. 21, p. 231-249.

———, Takenouchi, S. and Shoji, T. (1978) Mineralogy of deep sea manganese nodules and synthesis of manganese oxides: implication to genesis and geochemistry. *Mining Geol.*, vol. 28, p. 405-420.